[Northeast Journal of Complex Systems (NEJCS)](https://orb.binghamton.edu/nejcs)

Volume 4
Number 1 *Special Issue: NERCCS 2022 Papers*
Article 3

March 2022

Representing and Analyzing the Dynamics of an Agent-Based Adaptive Social Network Model with Partial Integro-Differential Equations

Hiroki Sayama
Binghamton University, SUNY, sayama@binghamton.edu

Representing and Analyzing the Dynamics of an Agent-Based Adaptive Social Network Model with Partial Integro-Differential Equations

Hiroki Sayama[1,2]

[1] Center for Collective Dynamics of Complex Systems

Binghamton University, State University of New York, Binghamton, NY, USA

[2] Waseda Innovation Lab, Waseda University, Tokyo, Japan

sayama@binghamton.edu

Abstract

We formulated and analyzed a set of partial integro-differential equations that capture the dynamics of our adaptive network model of social fragmentation involving behavioral diversity of agents. Previous results showed that, if the agents' cultural tolerance levels were diversified, the social network could remain connected while maintaining cultural diversity. Here we converted the original agent-based model into a continuous equation-based one so we can gain more theoretical insight into the model dynamics. We restricted the node states to 1-D continuous values and assumed the network size was very large. As a result, we represented the whole system as a set of partial integro-differential equations about two continuous functions: population density and connection density. These functions are defined over both the state and the cultural tolerance of nodes. We conducted numerical integration of the developed equations using a custom-made integrator implemented in Julia. The results obtained were consistent with the simulations of the original agent-based adaptive social network model we previously reported, confirming the robustness of the original finding. Specifically, when the variance of cultural tolerance d is large enough, the population with low d maintains the original clusters of cultures/opinions, while the one with high d tends to come to the center and connect culturally distant groups. Parameter dependence of the model behavior was also revealed through systematic numerical experiments.

1 Introduction

Social fragmentation and opinion polarization are the major social problems these days. They are partly driven by the advanced personalized information communication tools, such as social media and smartphones, on which people choose only such information sources that match their preference. While there are many recent studies on social fragmentation [1–9], most of the earlier studies typically considered only two societal outcomes: (1) fragmented society with many disconnected, incompatible social clusters and (2) well-connected society in which cultural/opinion states of individuals are homogenized. From a viewpoint of promoting creativity and innovation, however, the latter societal state (well-connected homogenization) is not any better than social fragmentation either, because of the loss of informational diversity it implies.

To seek the possibility of the third alternative social state that maintains *both* social connectivity and cultural/opinion diversity, we had proposed an agent-based adaptive social network model that incorporated behavioral diversity of nodes (agents) [10]. This model showed that, when the cultural tolerance levels of agents were diversified within society, social evolution could lead to a culturally diverse yet structurally connected state [10], which was not reported in the earlier literature of social fragmentation. However, this model was entirely computational and the simulation experiments were done with relatively small-sized network topologies, and hence it did not provide much theoretical insight into how a much larger social network might behave according to the same model assumptions.

In the present study, we have formulated and analyzed a set of partial integro-differential equations (PIDEs) [11] that collectively capture the essential dynamics of the aforementioned agent-based adaptive social network model. Numerical integration of the model equations produced the results that were consistent with previous results obtained using the agent-based model (ABM), which confirms the robustness of the original finding that behavioral diversity in cultural tolerance levels could help achieve culturally diverse yet connected society. In the rest of the paper, we will describe the original model (Section 2), the newly developed equation-based model (Section 3), the method for numerical integration (Section 4), numerical simulation results (Section 5), and then conclusions with limitations of the work and future directions (Section 6).

2 Original Agent-Based Model

The original agent-based adaptive social network model described social network evolution in which cultural information was shared among agents (nodes) and the weights of their connections (edges) were updated according to acceptance or rejection of shared cultural information [12, 13]. In this original model, each agent had a 10-dimensional numerical vector v_i as its cultural/opinion state, with i being the node ID. In each iteration, each agent would randomly choose one neighbor j from its out-neighbors by using the (normalized) edge weight w_{ij} as the selection probability and obtain the chosen neighbor's cultural state v_j as an input. Agent i would accept the received input with the following acceptance probability

$$P_A = \left(\frac{1}{2}\right)^{\frac{|v_i - v_j|}{d}}, \quad (1)$$

where d is the cultural tolerance level. If the input was accepted, then agent i's state would be updated as follows:

$$v_i \to (1 - r_s)v_i + r_s v_j \quad (2)$$

If the input was rejected, there would be no change to agent i's state. The acceptance/rejection of the input would also update the edge weight from i to j as follows (acceptance: $+$; rejection: $-$):

$$w_{ij} \to \text{logistic}(\text{logit}(w_{ij}) \pm r_w) \quad (3)$$

When all the agents did the above in a randomized order, that constituted one iteration in a simulation. This model included three parameters for agents' behaviors: d (cultural tolerance level), r_s (rate of cultural state change), and r_w (rate of edge weight change). In the original study presented in [12, 13], the same parameter values were uniformly applied to all the agents within a social network. By introducing behavioral diversity into this ABM, we previously demonstrated that, if the agents' cultural tolerance levels were diversified within society, the social network could remain connected while still maintaining cultural diversity (Fig. 1) [10]. This was not observed in other more conventional network models of social fragmentation.

3 New Model: Partial Integro-Differential Equations

In the current study, we have converted the rather complex, discrete, *if-then*-rule-based original ABM into a smooth, continuous, analytically tractable equation-based one so that we can gain more theoretical insight into the model dynamics. To make it easier to represent the configuration of the network that involves heterogeneity in behavioral traits of nodes, we have restricted the attributes and states of each node to one-dimensional continuous values and have assumed that the size of the network is very large, which allows for continuous representation. As a

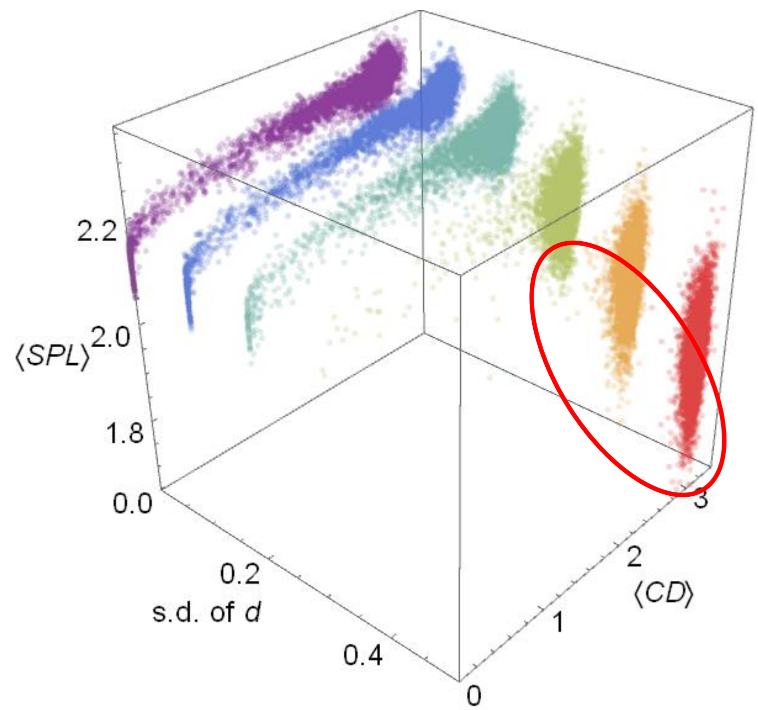

Figure 1: Simulation results of the original agent-based adaptive social network model (from [10]; slightly revised). This 3D scatter plot shows the effect of the diversity, or standard deviation (s.d.), of the cultural tolerance level (d) on two outcome measures ($\langle CD \rangle$, average cultural difference, and $\langle SPL \rangle$, average shortest path length) in the final network configuration. Each dot represents a result of one simulation run, colored according to the s.d. of d. The results marked by a tilted red ellipse show the structurally connected yet culturally diverse social states (i.e., small $\langle SPL \rangle$ and large $\langle CD \rangle$), which occur only when d is sufficiently diversified.

result, we have represented the whole system as a set of PIDEs about just two continuous state functions: population density function $p(v, d, t)$—density of nodes with opinion v and cultural tolerance d at time t, and connection density function $c(v, u, d_v, d_u, t)$—density of directed edges from nodes with opinion v and cultural tolerance d_v to nodes with opinion u and cultural tolerance d_u at time t. Note that c is asymmetric between v and u (and also between d_v and d_u). p is a probability density function since the total number of nodes remains constant, whereas c is not a probability density function. These functions are defined over a multidimensional domain made of the node state (v, u) and the cultural tolerance (d) of nodes involved. We also have assumed that other node attributes, r_s (cultural state change rate) and r_w (edge weight change rate), were fixed and homogeneous across all nodes because we previously found that their diversity would not have significant effects on the overall system behavior [10].

The basic strategy we took in converting the original ABM to PIDEs was to "count" and write down how many times acceptance/rejection occurs between agents with specific attributes (current opinion and cultural tolerance), and then represent the cultural state/edge weight changes according to the result of such counting as migration and local reaction in continuous space [11]. To do this, we first define the following formulas:

$$c_{v,d_v} = \frac{\int c \, \mathrm{d}d_u}{\int \int c \, \mathrm{d}d_u \mathrm{d}u} \tag{4}$$

$$P_a(x, d) = \left(\frac{1}{2}\right)^{\frac{|x|}{d}} \tag{5}$$

Eq. (4) represents the normalized probability density function of connectivity from a node with opinion v and cultural tolerance d_v to a neighbor with opinion u (irrespective of the neighbor's cultural tolerance d_u). Eq. (5) is the acceptance probability function for opinion difference $|x|$ and cultural tolerance d.

Using the above formulas, the probability for a node with opinion v and cultural tolerance d_v to accept an opinion coming from its neighbor with opinion u can be written as $c_{v,d_v} P_a(v - u, d_v)$, and such acceptance also causes the drift of opinion v toward $(1 - r_s)v + r_s u$, according to Eq. (2). The direction and magnitude of the drift are thus given by $(1 - r_s)v + r_s u - v = r_s(u - v)$. By integrating the product of these quantities over u, we obtain the overall trend of migration of p for nodes with opinion v and cultural tolerance d_v, as follows:

$$T_p(v, d_v) = \int c_{v,d_v} \, P_a(v - u, d_v) \, r_s(u - v) \, \mathrm{d}u \tag{6}$$

We incorporate this trend in the migration term and add another term for stochastic diffusion in a standard transport equation [11], to obtain the following first key equation of our PIDE model in terms of p:

$$\frac{\partial p}{\partial t} = D_p \frac{\partial^2 p}{\partial v^2} - \alpha \frac{\partial}{\partial v} \left[p \, T_p(v, d_v) \right] \tag{7}$$

Meanwhile, connection density function c also drifts along the v axis after the acceptance of a neighbor's opinion, because the opinion state v of the source nodes of involved edges changes due to the acceptance. The overall trend of this drift is given by

$$T_c(v, u, d_v, d_u) = P_a(v - u, d_v) \, r_s(u - v), \tag{8}$$

which is similar to $T_p(v, d_v)$ but does not involve the integrals because c is explicitly defined over a two-dimensional opinion space (v, u) (in addition to (d_v, d_u)). Finally, we note that c also increases or decreases locally after acceptance or rejection of a neighbor's opinion. The rate of such connectivity changes can be written down as

$$\begin{aligned} R_c(v, u, d_v, d_u) = & \,(1 - P_a(v - u, d_v)) \left(\text{logistic}(\text{logit}(c) - r_w) - c\right) \\ & + P_a(v - u, d_v) \left(\text{logistic}(\text{logit}(c) + r_w) - c\right), \end{aligned} \quad (9)$$

where the first term on the right-hand side is the probability of rejection times the edge weight decrease (per Eq. (3)) and the second term the probability of acceptance times the edge weight increase (again, per Eq. (3)).

By incorporating the above two functions in the migration and local reaction terms and adding another term for stochastic diffusion along v and u, we obtain the following second key equation of our PIDE model in terms of c:

$$\frac{\partial c}{\partial t} = D_c \left(\frac{\partial^2 c}{\partial v^2} + \frac{\partial^2 c}{\partial u^2} \right) + \beta c\, R_c(v, u, d_v, d_u) - \gamma \frac{\partial}{\partial v} \left[c\, T_c(v, u, d_v, d_u) \right] \quad (10)$$

Eqs. (7) and (10) collectively represent the continuous dynamics of population and connection densities based on the assumptions used in the original ABM. These equations are a concrete demonstration of how one can convert rule-based complex ABM rules into continuous mathematical equations.

4 Numerical Integration Method and Conditions

The developed PIDEs are rather complex because they involve double integrals in Eq. (4), which is used inside yet another integral in Eq. (6), and also because the two dependent variables p and c have different domains with different dimensionalities (i.e., p is over v, d and t, while c is over v, u, d_v, d_u and t). Most of the readily available PDE solvers cannot handle such complicated equations. We therefore have implemented a custom-made numerical integrator in Julia 1.7.1[1] by straightforward spatial discretization and a simple Euler forward method. The ranges and the resolutions of discretization of the independent variables used for numerical integration are as follows:

- v, $u \in [-5, 5]$, with Δv, $\Delta u = 0.1$
- d_v, $d_u \in [0, 2]$, with Δd_v, $\Delta d_u = 0.1$

[1] The code is available from the author upon request.

- $t \in [0, 50]$, with $\Delta t = 0.01$

The main experimental parameters varied are the following:

- Standard deviation of the distribution of cultural tolerance d: $\sigma(d) \in [0.1, 1.0]$
- Diffusion coefficients $D_p = D_c \in [0.003, 0.03]$ (The two diffusion coefficients were assumed to be the same for simplicity.)

Other settings are as follows:

- Mean of $d = 0.5$
- $r_s = r_w = 0.5$ (constant with no variation)
- $\alpha = \beta = \gamma = 1$
- Cut-off spatial boundary conditions

These parameter settings are consistent with those used in the original ABM [10], except for the diffusion coefficients that did not exist explicitly in the original ABM. The diffusion terms in the PIDE model represent aggregated stochastic behaviors of the agents.

The initial condition of p was set with a mixture of two multivariate Gaussian distributions with $\sigma(v) = 0.5$ and $\sigma(d)$ experimentally varied as described above. Their peaks were separated by 3.0 around the origin along the v axis (Fig. 2, top left), to represent two initially separated opinion clusters (this setting was used in the original ABM-based study [10]). The height of the peaks was adjusted to make p a valid probability distribution. The initial condition of c was set with a mixture of two multivariate Gaussian distributions with $\sigma(v) = \sigma(u) = 0.5$ whose peaks were separated by 3.0 around the origin along both the v and u axes, *plus* another mixture of two multivariate Gaussian distributions whose peaks were positioned along the opposite diagonal in the v-u space (Fig. 2, top right and bottom two). The heights of those pairs of the peaks were set to 1.0 and 0.3, respectively, to represent strong and weak connections within and between the initial two opinion clusters, respectively.

5 Results

Figure 3 shows the final states of population density function $p(v, d)$ and connection density function $c(v, u, d_v, d_u)$ at $t = 50$ for three different values of diffusion coefficients ($D_p = D_c = 0.003$ (top), 0.01 (middle), and 0.03 (bottom)) when the diversity of cultural tolerance d is low ($\sigma(d) = 0.1$). The diffusion represents the

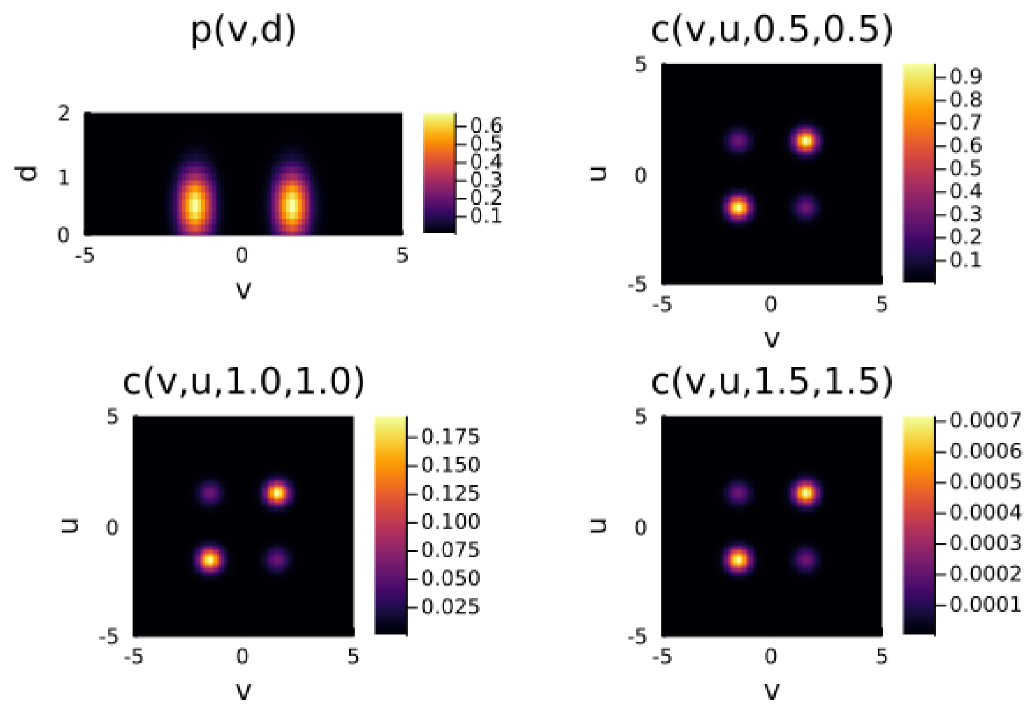

Figure 2: Initial condition of p (top left) and c (top right and bottom two) used in numerical integration. $\sigma(d) = 0.5$. Note that the initial condition of c was actually defined over a four-dimensional space (v, u, d_v, d_u). The three plots given here are only slices of the true distribution at $d_v = d_u = 0.5$, 1.0, and 1.5.

Table 1: Summary of parameter dependence of final states. Rows represent different values of cultural tolerance diversity ($\sigma(d)$) while columns represent different values of diffusion coefficients (D_p and D_c).

$\sigma(d)$	$D_p = D_c = 0.003$	$D_p = D_c = 0.01$	$D_p = D_c = 0.03$
0.1	Two clusters	One cluster	One cluster
0.2	Two clusters	One cluster	One cluster
0.3	Two clusters	Two clusters connected	One cluster
0.4	Two clusters	Two clusters connected	One cluster
0.5	Two clusters	Two clusters connected	One cluster

stochastic nature of agents' behaviors in this otherwise deterministic PIDE model. If diffusion is weak, the network remains separated in the initial two opinion clusters (Fig. 3 top). If diffusion is stronger, however, the two initial opinion clusters become blurred and merge into a single cluster (Fig. 3 middle and bottom). This corresponds to the typical social fragmentation transition that has been reported in many earlier models.

Meanwhile, when the diversity of cultural tolerance d is high enough, a different social state emerges. Figure 4 shows the final states of population density function $p(v, d)$ and connection density function $c(v, u, d_v, d_u)$ at $t = 50$ for three different values of diffusion coefficients ($D_p = D_c = 0.003$ (top), 0.01 (middle), and 0.03 (bottom)) when the diversity of cultural tolerance d is high ($\sigma(d) = 0.5$). The new social state is observed in the scenario with intermediate diffusion strength (Fig. 4 middle, $D_p = D_c = 0.01$), in which agents with greater cultural tolerance (d) approached the center and began connecting the two opinion clusters while agents with smaller d remained holding their original opinions. This resulted in a "frown ($\frown$)"-like shape of the $p(v, d)$ distribution, which represents diverse yet connected social networks. Such social states were not reported in conventional social fragmentation studies.

Table 1 presents an overview of parameter dependence of the model behavior obtained from numerical simulations with selected parameter values. It shows that social fragmentation transition occurs consistently between low stochasticity scenarios (= weak diffusion; Table 1 left column) and high stochasticity scenarios (= strong diffusion; Table 1 right column). However, the third social state ("Two clusters connected") emerges in moderate stochasticity scenarios (Table 1 center) when the behavioral diversity $\sigma(d)$ is increased to 0.3 or above.

Figure 5 shows more detailed results obtained from finer parameter sweep ex-

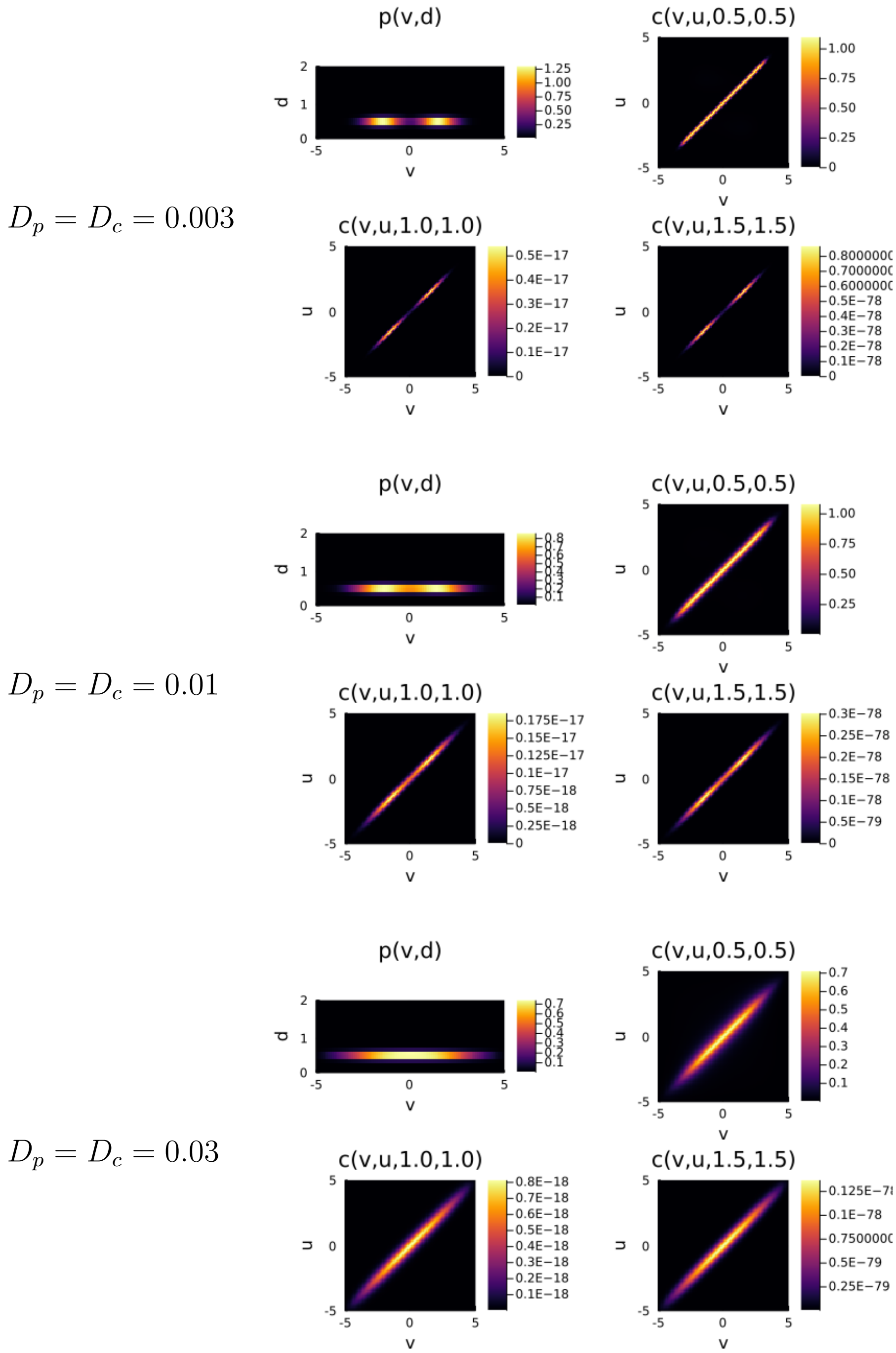

Figure 3: Final states of p and c at $t = 50$ when the diversity of cultural tolerance is low ($\sigma(d) = 0.1$). Results with three different diffusion coefficient values are shown. As the diffusion coefficients were varied, the model exhibited typical social fragmentation transition between two separated clusters (top) and a single unified cluster (bottom).

$D_p = D_c = 0.003$

$D_p = D_c = 0.01$

$D_p = D_c = 0.03$

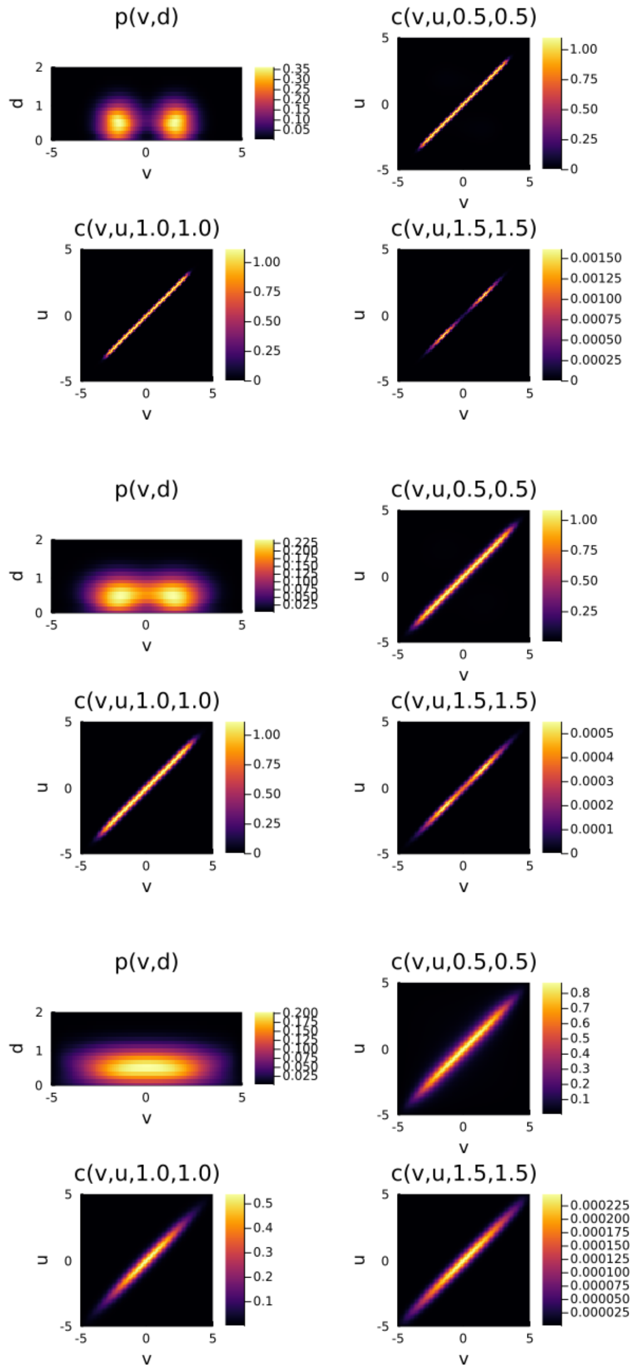

Figure 4: Final states of p and c at $t = 50$ when the diversity of cultural tolerance is high ($\sigma(d) = 0.5$). Results with three different diffusion coefficient values are shown. In this case, there appeared a new third state (middle; $D_p = D_c = 0.01$) in which agents with greater cultural tolerance (d) approached the center and began connecting the two opinion clusters while agents with smaller d remained holding their original opinions.

periments in which the final states of $p(v, d)$ (Fig. 5 top) were automatically classified into three categories using morphological image analysis (Fig. 5 bottom). Specifically, the gray-scale image of each final state of p was binarized at a 50% gray-level threshold and then the number of morphological components (connected regions) was counted. The patterns that had only one morphological component were further analyzed to assess the curvature of the bottom edge of the component. If it was substantially concave to exhibit the "frown ($\frown$)"-like shape, then the pattern was classified as "two clusters connected" (shown in yellow in Fig. 5 bottom).

Table 1 and Figure 5 visually represent a rough "phase space" of the developed PIDE model with regard to the behavioral diversity and stochasticity of agents. Interestingly, these results were also consistent with the simulation results of the original ABM reported in [10] in that $\sigma(d) \geq 0.3$ causes the third social state (see Fig. 1). This quantitative agreement of the results between two completely different modeling frameworks (ABM and PIDE) successfully demonstrates the validity and robustness of the numerical findings obtained in these studies.

6 Conclusions

In this paper, we have developed and analyzed a continuous equation-based version of the adaptive social network model of cultural/opinion dynamics. The developed PIDE model's behavior and parameter dependence were studied using a custom-made numerical integrator, which showed consistent results with what was found earlier using a computational network ABM. The main finding obtained in both models is that, when the cultural tolerance levels of constituents are diverse enough ($\sigma(d) \geq 0.3$), the adaptive social network can self-organize into a configuration with multiple well-established opinion clusters together with bridges that connect them. This is a possible alternative third state of society that goes beyond complete fragmentation or complete homogenization, the two only possible outcomes studied in typical social fragmentation models. Additional insights gained from the PIDE model include the role of stochasticity (diffusion) as the main factor of social fragmentation transition and the overall "phase space" structure of social evolution outcomes that depend on the agents' stochasticity and behavioral diversity.

This work is also a successful demonstration of the possibility and practicality of describing the dynamics of a complicated network ABM in continuous PIDEs. Such model conversion can be a useful practice for complex systems modeling and analysis, as the two modeling methodologies offer complementary analytical tools and insights.

This study still has many limitations. Due to the high computational demand from numerical integration of multidimensional PIDEs, the resolution of spatial discretization was not high; we had to use a rather large interval, 0.1, to discretize

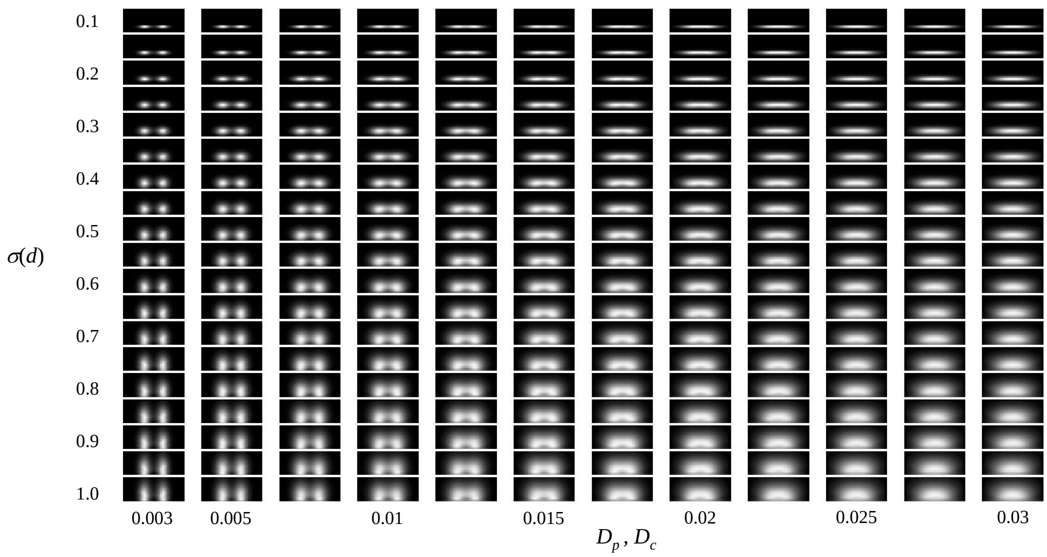

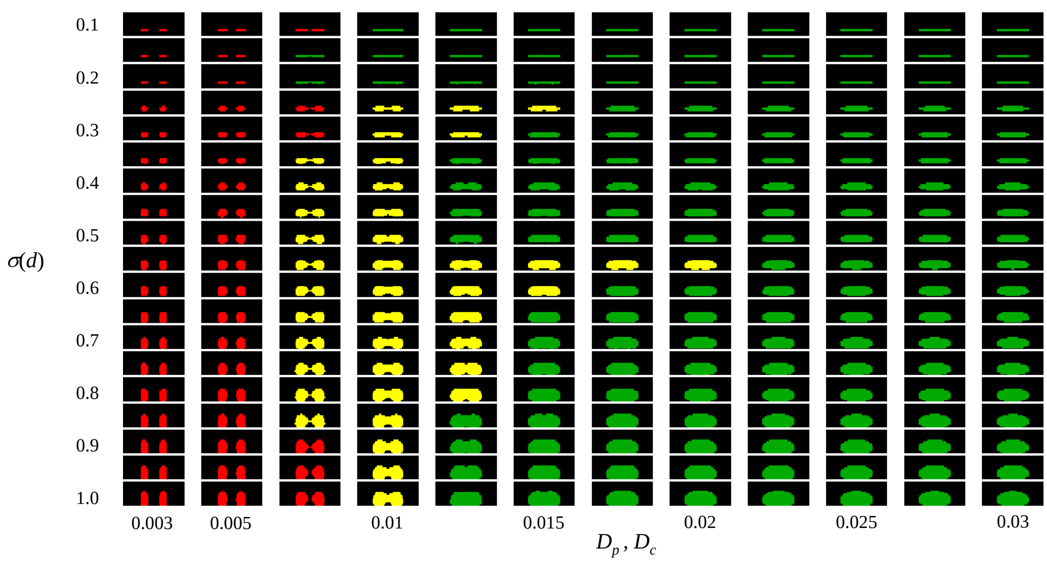

Figure 5: Results of finer parameter sweep experiments. Final states of $p(v, d)$ at $t = 50$ are shown for various values of $\sigma(d)$ and $D_p(= D_c)$. Top panel: Final states of p shown as gray-scale heat maps. Bottom panel: Final states of p binarized and then classified into three categories (red: two clusters; yellow: two clusters connected; and green: one cluster) using morphological image analysis (see text for details).

the v, u and d spaces. Also, the numerical parameter sweep conducted so far was still relatively coarse. In order to obtain a better understanding of the model's parameter dependence, we would need to carry out a greater number of numerical integrations. These tasks would naturally require substantial computational power and resources. Also, the characterization of final configurations remained largely categorical and qualitative (i.e., "two clusters", "two clusters connected", and "one cluster"). It would be desirable to develop and use a more objective, quantitative measure to characterize the final state of the population density function in order to derive more rigorous conclusions. Finally, there are still many more mathematical/algebraic analyses that need to be done on the proposed PIDE model, such as finding (non-homogeneous) stationary solutions and conducting stability analysis of those solutions. Such mathematical analyses may provide a deeper understanding of how and why the observed model behaviors occur for specific parameter values and settings.

Acknowledgments

We thank Junichi Yamanoi for his contribution to the original ABM-based study on which the present study is based. This work was supported by JSPS KAKENHI Grant Number 19H04220.

References

[1] Holme, P. & Newman, M. E. (2006). Nonequilibrium phase transition in the coevolution of networks and opinions. Physical Review E, 74(5), 056108.

[2] Centola, D., Gonzalez-Avella, J. C., Eguiluz, V. M., & San Miguel, M. (2007). Homophily, cultural drift, and the co-evolution of cultural groups. Journal of Conflict Resolution, 51(6), 905-929.

[3] Kozma, B., & Barrat, A. (2008). Consensus formation on adaptive networks. Physical Review E, 77(1), 016102.

[4] Böhme, G. A., & Gross, T. (2011). Analytical calculation of fragmentation transitions in adaptive networks. Physical Review E, 83(3), 035101.

[5] Bakshy, E., Messing, S., & Adamic, L. A. (2015). Exposure to ideologically diverse news and opinion on Facebook. Science, 348(6239), 1130-1132.

[6] Bail, C. A., Argyle, L. P., Brown, T. W., Bumpus, J. P., Chen, H., Hunzaker, M. B. F., Lee, J., Mann, M., Merhout, F., & Volfovsky, A. (2018). Exposure to

opposing views on social media can increase political polarization. Proceedings of the National Academy of Sciences, 115(37), 9216-9221.

[7] Sayama, H. (2020). Enhanced ability of information gathering may intensify disagreement among groups. Physical Review E, 102(1), 012303.

[8] Blex, C., & Yasseri, T. (2020). Positive algorithmic bias cannot stop fragmentation in homophilic networks. Journal of Mathematical Sociology, 1-18.

[9] Sasahara, K., Chen, W., Peng, H., Ciampaglia, G. L., Flammini, A., & Menczer, F. (2021). Social influence and unfollowing accelerate the emergence of echo chambers. Journal of Computational Social Science, 4(1), 381-402.

[10] Sayama, H., & Yamanoi, J. (2020). Beyond social fragmentation: Coexistence of cultural diversity and structural connectivity is possible with social constituent diversity. In Proceedings of NetSci-X 2020: Sixth International Winter School and Conference on Network Science (p. 171). Springer Nature.

[11] Sayama, H. (2015). Introduction to the Modeling and Analysis of Complex Systems. Open SUNY Textbooks.

[12] Yamanoi, J., & Sayama, H. (2013). Post-merger cultural integration from a social network perspective: A computational modeling approach. Computational and Mathematical Organization Theory, 19(4), 516-537.

[13] Sayama, H., Pestov, I., Schmidt, J., Bush, B. J., Wong, C., Yamanoi, J., & Gross, T. (2013). Modeling complex systems with adaptive networks. Computers & Mathematics with Applications, 65(10), 1645-1664.